Macromolecules

pubs.acs.org/Macromolecules Article

# Adsorption Active Diblock Copolymers as Universal Agents for Unusual Barrier-Free Transitions in Stimuli-Responsive Brushes

Shuanhu Qi,* Leonid I. Klushin, Alexander M. Skvortsov, and Friederike Schmid

Cite This: *Macromolecules* 2021, 54, 2592−2603 Read Online

ACCESS | Metrics & More | Article Recommendations

**ABSTRACT:** We reconsider a recently proposed design for smart responsive brushes, which is based on a conformational transition in very dilutely embedded block copolymers with a surface active block (Qi et al., *Macromolecules* **53**, 5326, 2020). Under certain conditions, the transition acquires an unusual character: it remains very sharp, but the barrier separating the adsorbed and desorbed states disappears completely. We show that these features are very robust with respect to changing almost all system parameters: the lengths of the inert and active blocks of the minority chain, the brush length, its density, and its polydispersity. The only relevant condition is that the inert block of the minority chain is long enough to extend outside the brush density profile. We develop an analytical theory that predicts the relevant characteristics of the transition and verify it with Monte Carlo simulations. We also show that the surprising universality of the transition properties is rooted in an underlying connection to the force-induced desorption transition, which is known to combine the features of the first- and second-order transitions with a pretransition fluctuation growth accompanied by phase coexistence.

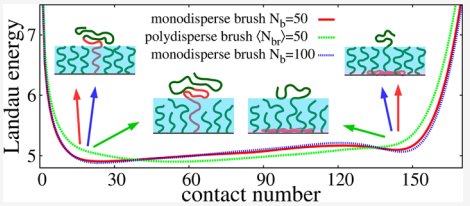




## INTRODUCTION

Polymer brushes with one end each chain grafted on a surface are ranked among the most promising systems in polymer science,[1−3] in particular for the modification of surfaces to, for example, tune wettability,[4] adsorption,[5,6] stabilization,[7−9] and lubrication.[10−12] In nanomedicine and material science, polymer brushes can be combined with stimuli-responsive components, such as active minority chains or reactive end-groups to create responsive polymer brushes, which become more interesting for drug delivery,[13] biosensors,[14] and smart surfaces.[15−20] Such a stimuli-responsive behavior usually relies on the phase transitions of the active component in the brush, and therefore, understanding their transition properties is previously crucial for the design of switch materials on demand.

One recently proposed way to create switchable surfaces is to embed a small number of adsorption active minority chains in an otherwise inert polymer brush.[21−23] The switching is associated with a conformational transition of the minority chains between two states, an adsorbed one where the chains are immersed in the brush and a desorbed one where the ends can extend outside the brush. For suitably chosen polymer characteristics, the transition is discontinuous.[24,25] This can be exploited for switching applications, e.g., for the design of switch sensors that could trigger a chemical reaction or catalytic processes in the solution by attaching specific groups at the end of the minority chain. Long minority chains provide benefits to get high yields of the reaction, as in this case where the catalytic agents and the reactants have a large probability to be in contact.

However, one crucial requirement for reliable switches is the absence of hysteresis, i.e., the energy barrier between the two switch states should be low. Recently, we have shown that it is possible to establish an independent control over the barrier height—without affecting other important transition characteristics such as the sharpness—by using block copolymers as switch chains that have an adsorption active inner (endgrafted) block and an inert outer block (with free end). For copolymers embedded in a monodisperse brush, we have shown that the barrier height even vanishes in the limit where the inert block has the same length than the brush chains. This clearly has technological potential. However, from a practical point of view, obtaining a precise control of block lengths in the copolymer is challenging, and making monodisperse brushes is even more challenging. In the present paper, we therefore reconsider the possibility of barrier-free transitions in more detail and address two key questions: (i) How robust is this feature with respect to variations in the characteristic properties of the system, i.e., brush polydispersity, grafting density, and copolymer block lengths? (ii) What is the underlying physics? To this end, we study the system by a theoretical analysis and Monte Carlo (MC) simulations.

**Received:** September 11, 2020
**Revised:** January 26, 2021
**Published:** March 2, 2021





https://dx.doi.org/10.1021/acs.macromol.0c02095
*Macromolecules* 2021, 54, 2592−2603

Our main results can be summarized as follows: In response to question (i), we find that sharp barrier-free transitions are universal features of block copolymer-based brush switches as long as the length of the two blocks exceeds certain critical values. In response to question (ii), we will show that the transition belongs to a class of "unusual" first-order transitions that are also observed in adsorbed endgrafted chains whose free end is subject to an external pulling force.[26−28] In the present case, the pulling force is provided by the osmotic repulsion due to the brush chains. This explains the universal and generic features that can be observed in our switch chain in a wide parameter range.

## THEORETICAL CONSIDERATION

We start analyzing the problem using a simplified mean field treatment. The system we are considering consists of a diblock copolymer chain of length $N$ with its active block grafted on a substrate in an inert monodisperse brush with grafting density $\sigma$ and chain length $N_{br}$. The chain length of the active block is written as $N_A$, and the inert block is $N_I$. The substrate imposes a short-ranged adsorption potential with strength $-\varepsilon$ (in the adsorption regime, $-\varepsilon$ is positive) over the active block monomers. We are interested in the case where $N_A > N_{br}$ so that the active block can switch between the exposed state and the adsorbed state by tuning the adsorption strength (see Figure 1), although the analysis of the transition is still valid for shorter active blocks, $N_A < N_{br}$, as well. We reproduce the theoretical thread proposed in ref 29 and particularly highlight the transition properties of diblock copolymer switches with $N_I > N_{br}$. To simplify the theoretical treatment, we assume that the brush chains are monodisperse so that the density profile is parabolic, although the main results remain valid even if the brush is formed by polydisperse chains.

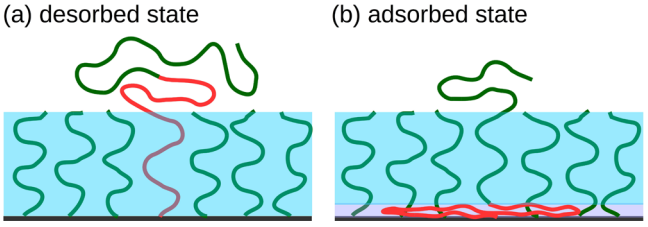


**Figure 1.** Schematic representation of the conformational transitions of the active block in a diblock copolymer chain in the desorbed state (a) and adsorbed state (b).

The free energy of a single diblock copolymer chain can be identified according to its conformation. We start by characterizing the adsorbed state not too close to the critical point of adsorption (to avoid significant finite-size corrections) in the absence of the brush. The free energy of the active block is extensive, and the free energy per monomer coincides with the chemical potential, which is a function of the adsorption strength, $-\mu(\varepsilon)$ ($-\mu$ is positive). The explicit form of the $\mu(\varepsilon)$ function is model-dependent.[30,31] Generally, at moderate adsorption strength, $\mu(\varepsilon) \approx -(\varepsilon - \varepsilon_c)^2$, where $\varepsilon_c$ is the critical point, while at stronger adsorption (upon approaching the saturation limit), $\mu(\varepsilon) \approx \varepsilon$. For an isolated diblock, the inert block forms a coil with zero free energy if one neglects the logarithmic corrections due to the surface impenetrability. Hence, one expects the adsorption properties of the diblock to be essentially unaffected by the presence of the inert block. Turning back to the original problem of a diblock surrounded by a monodisperse brush, we account for the effects due to crowded brush chains by means of the repulsive mean-field potential. In a monodisperse brush, the field is parabolic

$$V(z) = V_0\left(1 - \frac{z^2}{H^2}\right) \tag{1}$$

where

$$V_0 = \frac{3}{2}\left(\frac{\pi}{2}v\sigma\right)^{2/3} \tag{2}$$

is the potential on the surface, and $H \approx N_{br}(v\sigma)^{1/3}$ is the brush thickness. Note that according to the self-consistent field (SCF) theory, the value of the potential on the surface, eq 2, is determined solely by the combination of the excluded volume parameter $v$ and the brush grafting density $\sigma$ and depends neither on the brush chain length nor even on the brush polydispersity;[32−34] the latter fact is far from being obvious and will be exploited later on. In the case of moderate to strong adsorption, all active monomers are confined within the narrow adsorption layer much smaller than $H$, so the additional field energy carried by the active block is well approximated by $V_0N_A$. The free energy of the adsorbed active block in the presence of the brush is therefore written as $F_A = (V_0 + \mu)N_A$. The inert block has the conformation of a tail of length $N_I$ in a brush of length $N_{br}$. For further use, we need the free energy of an inert tail of arbitrary length $N_t$, which was studied in refs 21 and 24. Neglecting logarithmic corrections, the tail free energy is

$$F_t(N_t) = \begin{cases} V_0N_t, & N_t \le N_{br} \\ V_0N_{br}, & N_t \ge N_{br} \end{cases} \tag{3}$$

The existence of two branches is due to a sharp conformational transition of the guest chain in a monodisperse brush, from a perturbed coil at $N_t < N_{br}$ to a stem-crown structure for $N_t > N_{br}$ with a stem equal to the length of the brush chains, and a coil-like crown with $(N_t - N_{br})$ monomers residing beyond the brush profile and carrying no additional free energy.

We start the analysis assuming that the inert block is shorter than the brush chains, but the full length of the diblock is larger: $N_I < N_{br} < N_A + N_I$. Altogether, the free energy of the diblock copolymer chain in the fully adsorbed state is

$$F_{ads} = (V_0 + \mu)N_A + F_t(N_I) = (V_0 + \mu)N_A + V_0N_I \tag{4}$$

Next, we consider out-of-equilibrium partially adsorbed conformations of the diblock that are obtained by tearing the active block monomers off the adsorption layer, starting from the junction between the active and inert blocks, so that they become part of the tail with no surface contacts. We denote the number of torn-off monomers as $n$, with obvious conditions that $0 \le n \le N_A$. The nonequilibrium free energy as a function of $n$ is written similarly to eq 4

$$F(n) = (V_0 + \mu)(N_A - n) + F_t(N_I + n) \tag{5}$$

When all the monomers are torn off, we get the completely desorbed state with the free energy of

$$F_{des} = F_t(N_I + N_A) = V_0N_{br} \tag{6}$$

In the situation of interest here, the nonequilibrium free energy $F(n)$ initially grows linearly with the slope of $-\mu$ until the tail length equals $N_{br}$ when the tail free energy switches to


https://dx.doi.org/10.1021/acs.macromol.0c02095
Macromolecules 2021, 54, 2592−2603

the constant value branch (see eq 3). After that, $F(n)$ starts decreasing with the slope of $V_0 + \mu \leq 0$. Switching to the decreasing branch takes place at $n^* = N_{br} - N_I$, which defines the position of the maximum of $F(n)$, i.e., the barrier separating the two pure states (see Figure 2a). In a vicinity of the

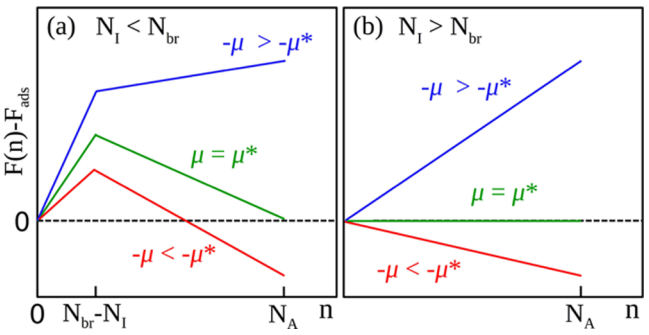


**Figure 2.** Cartoon showing the nonequilibrium free energy as a function of number of monomers removed from the adsorbed phase, $n$, in the case of a shorter block $N_I<N_{br}$ with $\mu^* \equiv \mu(\varepsilon^*)$ given by eq 7 (a) and in the case of a longer inert block $N_I>N_{br}$ with $\mu^* \equiv \mu(\varepsilon^*) = -V_0$ from eq 10 (b). Lower lines correspond to weak attraction: upper lines to strong attraction and middle lines to the transition point.

transition point, one of the states is equilibrium, while the other is metastable. One can also identify the spinodal conditions by equating the slope of the rising or decreasing branches to zero. The transition point is defined by the condition $F_{ads} = F_{des}$, which results in

$$\mu(\varepsilon^*) = -V_0 \frac{N_I + N_A - N_{br}}{N_A} \tag{7}$$

The barrier height at the transition is

$$U_{barrier} = F(n^*) - F(0) = V_0(N_{br} - N_I)\frac{N_I + N_A - N_{br}}{N_A} \tag{8}$$

It is clear that the nonequilibrium free energy $F(n)$ in our exposition served the same role as the Landau free energy as a function of the order parameter in a first-order transition scenario, in the sense that it allowed one to identify equilibrium and metastable states, to determine the transition point, and to quantify the barrier separating the two states. There are some conceptual differences between the two pictures that we would like to clarify. In a classical picture of the mean-field Landau free energy, the order parameter is a local quantity, and the two minima are separated by a barrier representing an unfavorable condition. In our case, the interfacial free energy is absent: this is a unique feature of a partially adsorbed flexible chain since the interface between the adsorbed and desorbed parts consists of a single monomer (a single point in idealized continuum models) and does not carry any additional free energy penalty. On the other side, our parameter $n$ playing the role of the order parameter is nonlocal and expresses the idea of forced out-of-equilibrium phase coexistence.

In the present work, we focus on the case where the inert block is longer than the brush chains, $N_I>N_{br}$. It turns out to be simultaneously the simplest, the most puzzling in its simplicity and universality, and perhaps, the most interesting from the fundamental and applied points of view.

The nonmonotonic behavior of the free energy $F(n)$ originated from switching between the two branches of the tail free energy (eq 3). Once the inert block is longer than $N_{br}$, only the second (constant) branch of $F_t(N_t)$ is in play, and the nonequilibrium free energy $F(n)$ simplifies to a linear function

$$F(n) = V_0 N_{br} + (V_0 + \mu)(N_A - n) \tag{9}$$

Depending on the adsorption parameter $\varepsilon$, three different scenarios can be identified. If the adsorption is strong, i.e., $-\mu(\varepsilon)>V_0$, then $F(n)$ increases monotonically and the minimum is located at $n = 0$, identifying the adsorbed state as the stable equilibrium. For weak adsorption $-\mu(\varepsilon)<V_0$, $F(n)$ decreases monotonically, the minimum at $n = N_A$ corresponding to the fully desorbed state. No metastable states are ever present. The linear $F(n)$ dependence strongly resembles Maxwell's construction, whereby the free energy of a phase-segregated state is taken as a linear combination of the free energies of two pure phases (see Figure 2b). However, it is achieved not in the macroscopic limit and is neglecting interfacial contributions; rather, it appears naturally from statistical mechanical results and accurately describes finite systems. In addition, the Landau free energy adopted here is conceptually different from the potential of mean force (PMF) between two particles in a fluid,[35,36] although they have much in common. For example, both are logarithms of a certain equilibrium distribution function and both are connected to the notion of the free energy as the measure of the equilibrium isothermal work. Indeed, Landau free energy can be understood as the potential of mean generalized force conjugate to the order parameter. However, they have different dependence on the system size and show different behaviors in the thermodynamic limit. In the case of the mean force between two particles, the system size is largely irrelevant;[35] on the other hand, the total Landau free energy is extensive and this is the origin of the nonanalytic behavior in the thermodynamic limit.

The transition point is defined by the following condition

$$-\mu(\varepsilon^*) = V_0 \tag{10}$$

At the transition, the nonequilibrium free energy is flat

$$U_{barrier} = 0 \tag{11}$$

All the partially adsorbed states carry the same statistical weight, resulting in barrier-free, anomalously large fluctuations. It follows from eq 10 that the transition point $\varepsilon^*$ is determined solely by $V_0$, which in turn depends only on the combination of the excluded volume parameter and the brush grafting density (see eq 2 and the discussion above). No effect of the block lengths and the brush length is expected.

Starting from eq 9, one can obtain a closed analytical expression for the partition function by summing a geometric progression

$$Z = \sum_{n=0}^{N_A} e^{-F(n)} = Z_0 \frac{1 - \exp[-(N_A + 1)x]}{1 - \exp(-x)}$$
$$= Z_0 \exp\left(-\frac{N_A}{2}x\right)\frac{\sinh\left(\frac{N_A + 1}{2}x\right)}{\sinh\left(\frac{x}{2}\right)} \tag{12}$$

where $Z_0 = \exp(-V_0 N_{br})$ is the adsorption-independent factor, and $x = V_0 + \mu(\varepsilon)$ vanishes at the transition point. The average number of the adsorption monomers is obtained as


https://dx.doi.org/10.1021/acs.macromol.0c02095
Macromolecules 2021, 54, 2592−2603

$$\langle m\rangle = -\frac{\partial \ln Z}{\partial \varepsilon} \simeq N_A \theta_{homo}(\varepsilon)\left[\frac{1}{2} - \frac{1}{2}\coth\left(\frac{N_A}{2}x\right) + \frac{1}{2N_A}\coth\frac{x}{2}\right] \quad (13)$$

where $\theta_{homo}(\varepsilon) = \frac{\partial \mu}{\partial \varepsilon}$ is the average adsorbed fraction for the adsorption-active homopolymer in the absence of any brush (see data in Figure 3 for $N_I = 0$) and certain simplifications

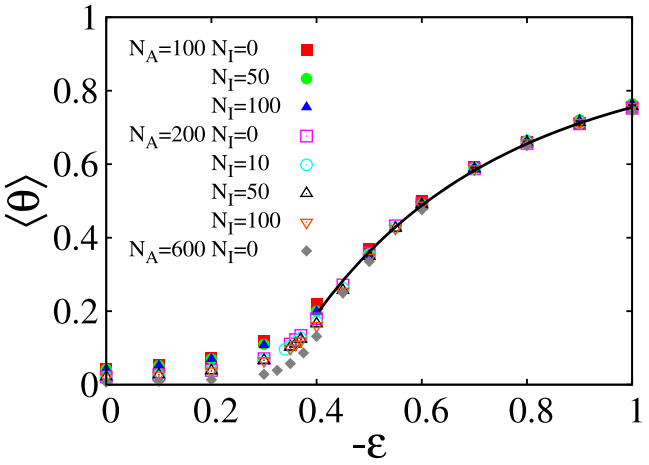


**Figure 3.** Average fraction of number of contacts as a function of adsorption strength $-\varepsilon$ for two different active block lengths $N_A$ = 100and 600 (filled symbols) and $N_A$ = 200 (empty symbols). The diblock copolymer interacts only with the surface; no brush is present. The continuous black line is the fitted line (see eq 16).

were made ($N_A + 1 \simeq N_A$). The quantity $\theta_{homo}$ is averaged over fluctuations in the number of contacts for a homopolymer of fixed length; however, we omit the averaging sign to avoid cumbersome notation. The number of contacts given by eq 13 is additionally averaged over the fluctuating length of the adsorbed part of the sticky block, which changes sharply near the transition point. For the purpose of comparing the theory to simulation results, the variable $x = V_0 + \mu(\varepsilon)$ can be approximated by its Taylor expansion around the transition point, $x = \theta_{homo}(\varepsilon^*)(\varepsilon - \varepsilon^*)$. In a very narrow vicinity of the transition, eq 13 simplifies to

$$\langle m\rangle \simeq \frac{N_A}{2}\theta_{homo}(\varepsilon^*) - \frac{N_A^2}{12}\theta_{homo}^2(\varepsilon^*)(\varepsilon - \varepsilon^*) \quad (14)$$

The variance of the number of contacts is obtained by another differentiation

$$\langle m^2\rangle - \langle m\rangle^2 = -\frac{\partial\langle m\rangle}{\partial\varepsilon} = -\frac{d\theta_{homo}}{d\varepsilon}\frac{N_A}{2}\left[1 - \coth\left(\frac{N_A}{2}x\right) + \frac{1}{N_A}\coth\frac{x}{2}\right] + \theta_{homo}^2(\varepsilon) \times \left[-\frac{N_A^2}{4\sinh^2\left(\frac{N_A}{2}x\right)} + \frac{1}{4\sinh^2\frac{x}{2}}\right] \quad (15)$$

The variance reaches a maximum value of $\frac{N_A^2\theta_{homo}^2(\varepsilon^*)}{12}$ at the transition point.

The transition width $\delta\varepsilon$ is inversely proportional to the steepness of the normalized adsorption curve $\langle\theta\rangle$ vs $\varepsilon$, where $\langle\theta\rangle = \langle m\rangle/N_A$ can be read off from eq 15, i.e., $\delta\varepsilon \approx 12N_A^{-1}$.

The fundamental relations of eq 10, eq 11, and $\delta\varepsilon \approx N_A^{-1}$ characterize the universal features of the phase transitions of the diblock copolymer switches with long inert blocks. It is clear that the transition point is affected only by the brush grafting density, the barrier is always absent, and the active block length effectively controls the transition sharpness. Although the above derivation assumed a monodisperse brush, we will demonstrate later through MC simulations that the universality still holds for polydisperse brushes.

To compare the theory predictions, eqs 13 and 15, to MC simulations, we need an explicit expression for $\theta_{homo}(\varepsilon)$, which is accomplished by fitting the MC data for isolated homopolymer chains (see Results of MC Simulations). The average adsorbed fraction in an isolated homopolymer shown in Figure 3 is to be identified with $\theta_{homo}(\varepsilon)$. In the range of interest, $0.4 \le -\varepsilon \le 1.4$, the function $\theta_{homo}(\varepsilon)$ is accurately described by an empirical fitting formula

$$\theta_{homo} \approx -2.872 + 7.418(-\varepsilon)^{1/2} - 4.257(-\varepsilon) + 0.466(-\varepsilon)^2 \quad (16)$$

This will be later utilized to generate theoretical curves according to eqs 13 and 15 in Figures 9b and 14, respectively.

## MC SIMULATIONS

In the following, we use coarse-grained off-lattice MC simulations to verify the idea proposed in the above section.[37,38] The MC simulations are performed in the canonical ensemble. The simulation box has a volume of $V = L_x \cdot L_y \cdot L_z$, where $L_x$, $L_y$, and $L_z$ are the side extensions along the $x$, $y$, and $z$ directions, respectively. To model an infinite polymer brush, we utilize periodic boundary conditions along the $x$ and $y$ directions and set impenetrable boundaries along the $z$ direction at $z = 0$ and $z = L_z$. Polymer chains in the system are discretized as monomer beads connected by Gaussian springs with the spring constant $3k_BT/a^2$, where $a$ is the statistical bond length (it also measures the size of a monomer), $k_B$ is the Boltzmann constant, and $T$ is the temperature. The solvent in the system is taken into account implicitly. Each polymer is grafted firmly with one of its ends on a plane at $z = z_0$, with the grafting points forming a simple squared lattice. The total number of lattice points is equal to the total number of polymer chains, and the lattice points are fixed in space. Here, $z_0$ is chosen much smaller than $a$ for practical purpose.[23] The impenetrable wall at $z = 0$ imposes a short-ranged attractive potential $U_{ads}(z)$ to the active monomers in the diblock copolymer chain. For simplicity, we set $U_{ads}$ as a step function, and it is characterized by the magnitude $-\varepsilon$ and the interaction range $0 \le z \le a$. Hereafter, we use $a \equiv 1$ as the length unit and $k_BT \equiv 1$ as the energy unit.

The total energy of the diblock copolymer and brush system has three contributions: the bonded energy $H_0$ due to the chain connection, the nonbonded monomer−monomer interaction $H_I$ from the excluded volume effect, and the adsorption energy $H_{ads}$ arising from the attraction between the substrate and the active monomers. The bonded interaction is the sum of the elastic energy from all bonds, and it can be


https://dx.doi.org/10.1021/acs.macromol.0c02095
Macromolecules 2021, 54, 2592−2603

expressed as $H_0 = \frac{3}{2}\sum_{\alpha j}(\mathbf{R}_{\alpha j} - \mathbf{R}_{\alpha,j-1})^2$, where $\alpha$ labels polymer chains, and $j$ labels monomers. The excluded volume interactions are expressed as a function of local density, i.e., $H_I = \frac{\nu}{2}\int d\mathbf{r}\hat{\rho}_t^2(\mathbf{r})$, where $\nu$ is the excluded volume parameter, $\hat{\rho}_t(\mathbf{r}) \equiv \sum_{\alpha j}\delta(\mathbf{r} - \mathbf{R}_{\alpha j})$ is defined as the local density, and the summation runs over all monomers in the system including both brush monomers and diblock copolymer monomers. The adsorption energy is written as $H_{ads} = \sum_j U_{ads}(z_j)$, where $z_j$ denotes the $z$ coordinate of the $j$th active monomer, and $j$ runs over all active monomers in the diblock copolymer chain.

In the simulation, we will consider both monodisperse and polydisperse brushes. For the monodisperse brush, we set all brush chains the same length $N_{br}$. To model polydisperse brushes, we sample the brush chains with their lengths, satisfying the Schulz−Zimm (SZ) distribution.[39,40] The continuous SZ distribution is a two-parameter function, which has the form of

$$P(N) = \frac{k^k N^{k-1}}{\Gamma(k)\langle N_{br}\rangle^k}\exp\left(-k\frac{N}{\langle N_{br}\rangle}\right) \quad (17)$$

where $k$ and $\langle N_{br}\rangle$ are the two free parameters tuning the shape of the of the distribution. Here, $\Gamma(k)$ is the gamma function. This SZ distribution is normalized $\int_0^\infty dNP(N) = 1$. The first-order moment is calculated as $\int_0^\infty dNNP(N) = \langle N_{br}\rangle$, showing that $\langle N_{br}\rangle$ is the number-averaged chain length. The second-order momentum is given by $\int_0^\infty dNN^2P(N) = \langle N_{br}\rangle^2\frac{k+1}{k}$, leading to the relation between the weight-averaged chain length and number-averaged chain length $N_w/\langle N_{br}\rangle = (k+1)/k$.[41] Thus, $k$ measures the polydispersity of the brush chains, and a small $k$ corresponds to a large polydispersity.

In the MC simulations, local densities are extracted from the position of each bead by using the particle-to-mesh scheme, which is a way to smoothen the density.[37,38,42] In the current work, we use the zeroth-order scheme, i.e., monomers are smeared out to its nearest neighbor cell. For the details of this scheme and other higher-order schemes, we refer the readers to refs 28 and 42. In practice, chain lengths are sampled according to the discretized SZ distributions, which match their continuous counterpart with the zero-, first-, and second-order moments within the chosen errors (e.g., less than 2%).[43]

In the present study, we set $L_x = L_y = 40$ and $L_z = 200$. The length of $L_z$ is large enough that no confinement effect is observed. We set the excluded volume parameter $\nu = 1$, which corresponds to a good solvent condition with the Flory−Huggins parameter $\chi = 0$. We choose $\sigma = 0.1$ and $\sigma = 0.2$ alternately to show that the results are qualitatively independent of $\sigma$. For the polydisperse brush, we use $k = 7$ to represent generally a polydisperse brush, and this corresponds to the moderately polydisperse case with approximately a linear density distribution.

MC simulations were carried out according to the standard Metropolis criterion.[44] After all chains are generated, they are grafted to the lattice points randomly except for the diblock copolymer chain, which is always grafted at a lattice point that is chosen to be near the center of the lattice plane, although its specific location does not affect the final results. This means that in the case of polydisperse brushes, chains with different lengths are arranged at the grids in a random way. In all the simulations, $6 \times 10^5$ MC steps per monomer were performed to equilibrate the system and another $4 \times 10^5$ MC steps per monomer to extract statistical averages. To improve the statistics, during the process of evaluating the physical quantities, additional $10^8$ MC steps per monomer updating the single diblock copolymer chain were performed. Final statistical quantities were obtained by averaging the results from eight separate independent runs with different arrangements of chains at the grafting points, and from these results, errors were estimated. We note that the obtained errors were smaller or comparable to the size of the symbols in the figures, so the error bars were discarded.

To characterize the transition properties of the active block, we focus mainly on two different quantities: the average number of contact $\langle m\rangle$ and the distribution of number of contacts $P(m)$; from which the transition width is analyzed, the transition point and energy barrier are extracted. The number of contact $m$ is defined as the number of active monomers that are located in the adsorption layer. The transition width is related to the sharpness of the profile $\langle m\rangle$ as a function of the adsorption strength $-\varepsilon$. A sharp profile of $\langle m\rangle$ results in a small transition width. The distribution $P(m)$ is defined as the probability to find the number of contact $m$, and $P(m)$ is obtained by counting the number of times that $m$ contacts are found, divided by the total number of sampling.

At the transition point, the adsorption state and the desorbed state coexist. For the conventional first-order transitions, two coexisting states are separated by an energy barrier, and therefore, the distribution $P(m)$ has a bimodal structure. The transition point in this case is defined as the specific adsorption strength $-\varepsilon^*$ when the two maxima presented in $P(m)$ are equal. The energy barrier is obtained through the Landau free energy $U(m) = -\ln P(m)$ at the transition point as the energy barrier between the two minima. In contrast, for the unconventional first-order transitions particularly studied in this work, no energy barrier appears at the transition point. In this case, the transition point is defined when $P(m)$ has a large flat region corresponding to the zero energy barrier in $U(m)$.

## RESULTS OF MC SIMULATIONS

To test the theoretical predictions, we focus on the conformational transition of the active block of a single diblock copolymer in a brush with an arbitrary length of the active block $N_A$ and the inert block longer than the brush-forming chains $N_I > N_{br}$ in the monodisperse case and $N_A > 2.5\langle N_{br}\rangle$ in the moderately polydisperse brush (Zimm−Schultz distribution with $k = 7$).[45,46]

**Continuous Transition in an Isolated Diblock without a Brush.** We first show the phase behavior of a single endgrafted diblock copolymer on a bare substrate (no brush) for comparison. Theoretical and simulation studies have shown that a single grafted active homopolymer chain subjected to a short-ranged adsorption from the substrate undergoes a continuous phase transition. When an inert block is attached to the free end of the homopolymer chain, it becomes a diblock copolymer chain. However, the active block behaves as if no additional inert monomers are attached since the inert block does not impose a noticeable tearing force to the active monomers. In this situation, the phase transition behavior of the active block is similar to that of a homopolymer chain.

Figure 3 shows the ensemble average of the fraction of adsorption monomers $\langle\theta\rangle \equiv \langle m\rangle/N_A$ as a function of adsorption strength $-\varepsilon$. For $N_A = 100$, $N_A = 200$, and $N_A = 600$, $\langle\theta\rangle$ is a continuous monotonic function with a slowly


https://dx.doi.org/10.1021/acs.macromol.0c02095
Macromolecules 2021, 54, 2592−2603

increasing region followed by a rapidly increasing part. The symbols for different $N_I$ and the same $N_A$ collapse onto one curve, showing that the transition behavior does not depend on the length of the inert block. Weak finite chain length effects are observed with respect to $N_A$; for smaller $N_A$, the profile of $\langle\theta\rangle$ gradually smears out. On the other hand, at large $N_A$, a sharp crossover between the slowly increasing region and the rapidly increasing region can be seen. It can be expected that in the infinite chain limit $N_A\to\infty$, the order parameter $\langle\theta(\varepsilon)\rangle$ remains continuous, while its slope experiences a jump at the point $\varepsilon^* \approx -0.35$. Such a behavior of $\langle\theta(\varepsilon)\rangle$ indicates a continuous phase transition of a nearly mean-field type, which has been studied extensively in the case of a homopolymer.

The features of the phase transitions of the single grafted chains can also be investigated by studying the distribution of number of contact $P(m)$. If $(-\varepsilon)$ is small, then the average number of contact is small, corresponding to a narrow distribution of $P(m)$ with a large maximum in the small $m$ region (see Figure 4). With increasing $(-\varepsilon)$, the profile of

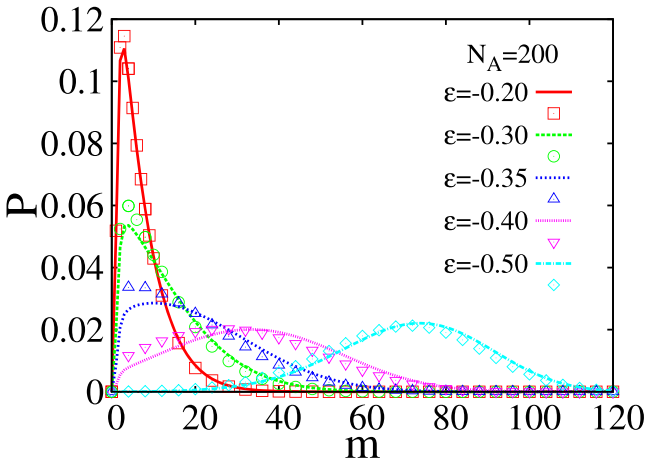


**Figure 4.** Distribution of number of contacts as a function of contact number $m$ at different adsorption strengths for homopolymer switches with $N_A = 200$ (lines) and diblock copolymer switches with $N_A = 200$ and $N_I = 100$ (empty symbols). In both cases, the transition point between the adsorbed state and the desorbed state is about $\varepsilon^* \approx -0.35$, which is equal to that obtained from the extrapolation in the infinite chain length limit.

$P(m)$ widens, but the location of its maximum remains close to the substrate, and this corresponds to the regime of slowly increasing $\langle\theta\rangle$. After crossing a threshold, the location of the maximum starts moving rapidly toward the large $m$ region. This corresponds to the regime where $\langle\theta\rangle$ increases rapidly in Figure 3. The crossover point between the two regimes is roughly consistent with the adsorption transition point obtained from the infinite chain extrapolation in Figure 3, $\varepsilon^* \approx -0.35$. It can be seen that with varying $-\varepsilon$, $P(m)$ always has just one maximum. The unimodal structure of $P(m)$ is also a signature of second-order phase transitions.

Figure 4 compares $P(m)$ for a single grafted homopolymer with $N_A = 200$ and a diblock copolymer chain with $N_A = 200$ and $N_I = 100$. If the adsorption strength is the same, then their distributions are approximately identical, indicating that the features of the continuous-phase transition do not depend on the length of the inert block.

**Phase Transitions: From Continuous to First-Order Type.** However, if the substrate is coated by an inert brush, then the nature of the phase transitions of the grafted single chain changes. For an active homopolymer chain in a monodisperse brush, the conformation transition of the homopolymer chain becomes sharp with a finite energy barrier at the transition point if the length of the active chain is longer than the brush chains. The sharp transition can be quantitatively verified from the curve of $\langle m\rangle$ as a function of $-\varepsilon$ where an abrupt change will happen at the transition point.

The curve for $N_I = 0$ in Figure 5 gives the profile of $\langle\theta\rangle$ for a homopolymer switch chain with $N_A = 100$, which is two times

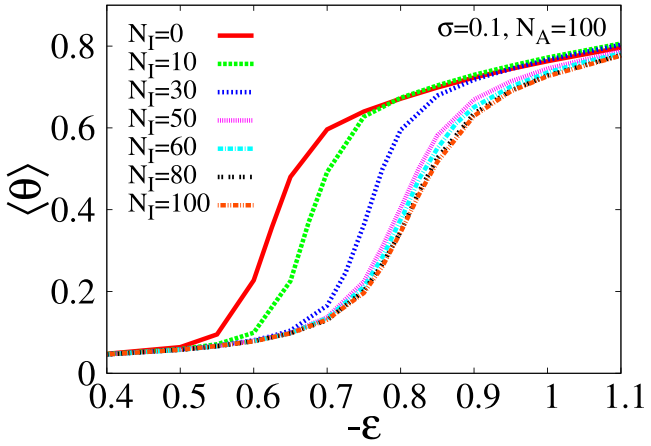


**Figure 5.** Average fraction of number of contacts for a single diblock copolymer in a monodisperse brush with active block length $N_A = 100$ and varying length of the inert block as a function of the adsorption strength. The length of the brush chains is $N_{br} = 50$, and the grafting density of the brush is chosen as $\sigma = 0.1$.

longer than the brush chains ($N_{br} = 50$). The sharp increase in $\langle\theta\rangle$ around $\varepsilon^* \approx -0.63$ indicates a first-order transition from the exposed state (at low $(-\varepsilon)$ to the adsorbed state (at high $(-\varepsilon)$), which is again smeared out due to finite chain length effects. With increasing length of $N_I$, the shape of $\langle\theta\rangle$ does not change, implying that the phase transitions for diblock copolymer switches are still of first order.

Depending on the length of $N_I$, one can identify two possible scenarios in the curves of $\langle\theta\rangle$. If $N_I<N_{br}$, then with increasing $N_I$, the curve $\langle\theta\rangle$ shifts horizontally toward a larger $(-\varepsilon)$ region, indicating an increase in the critical value $-\varepsilon^*$. This can be understood as follows: When $N_I$ becomes larger, the total number of inert monomers that have to be pulled into the brush during the phase transition increases, leading to the promotion of the adsorption energy $-\varepsilon^*$. If $N_I>N_{br}$, then there are always residual inert monomers residing outside the brush, the effective number of inert monomers involved in phase transitions is the same, and thus, the transition point becomes independent of $N_I$. In particular, for $N_I>N_{br}$, all curves almost collapse into a single master curve, indicating that the transition point and the transition width become independent of $N_I$.

To see the influence of $N_I$ on the energy barrier, we plot $U(m) = -\ln P(m)$ as a function of $m$ at the transition point for some specific $N_I$ in Figure 6. These curves can also be understood in terms of two scenarios depending on $N_I$ that are consistent to those shown in Figure 5. It is clearly seen in Figure 6 that with increasing $N_I$, the energy barrier decreases continuously to zero as $N_I$ approaches $N_{br}$. The energy barrier is always zero when $N_I>N_{br}$.


https://dx.doi.org/10.1021/acs.macromol.0c02095
Macromolecules 2021, 54, 2592−2603

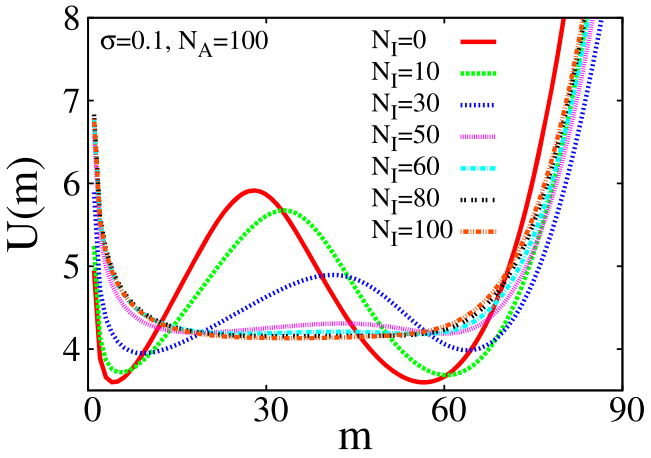


**Figure 6.** Landau free energy as a function of contact number $m$ for a single diblock copolymer in a monodisperse brush with some chosen length of the inert block $N_I$ at their corresponding transition point $-\varepsilon^*$. The length of the active block is fixed at $N_A = 100$. The length of the brush chains is $N_{br} = 50$, and the grafting density of the brush is chosen as $\sigma = 0.1$.

From Figures 5 and 6, we conclude that when an active polymer is immersed into a brush, its conformational transition becomes sharp and of first order. In particular, for diblock copolymer chains with inert blocks that are longer than the brush chains, the first-order transition becomes unconventional such that the energy barrier at the transition point vanishes.

**Universality of the Barrier-Free Transitions.** Now, we demonstrate that the barrier-free transitions discussed above are general, they can be observed in diblock copolymer switches if both the active block and inert block are longer than the brush chains, and the structure details of the brush chains are not relevant. For example, the adsorption curves only depend on $N_A$ and $\sigma$ and not on the values of $N_{br}$ or on the polydispersity of the brush.

Figure 7 plots $\langle\theta\rangle$ as a function of the adsorption strength ($-\varepsilon$) for single diblock copolymer chains in different monodisperse brushes and polydisperse brushes with $k = 7$.

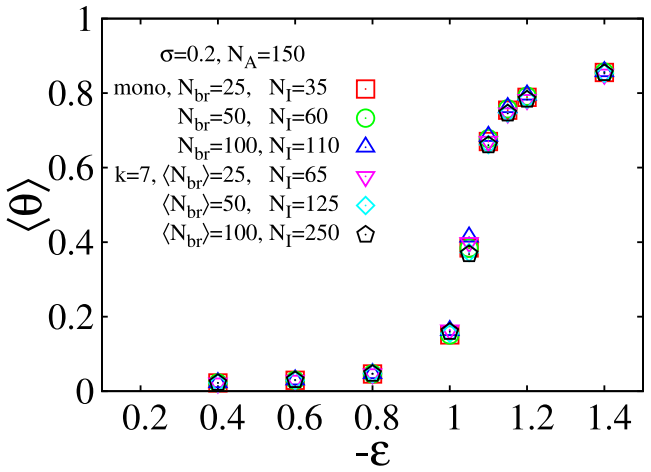


**Figure 7.** Average fraction of number of contact for diblock copolymer chains in monodisperse and polydisperse brushes with different setups of brushes and different lengths of $N_I$. The active block length is set at $N_A = 150$, and the grafting density of the brush is chosen as $\sigma = 0.2$.

For monodisperse brushes, we set the inert block 10 monomers longer than the brush chains, and in polydisperse brushes, the inert block is 2.5 times longer than the number-average length of the brush chains. These setups ensure that there are always inert block monomers staying outside the brush even in the strongly adsorbed state. It can be seen from Figure 7 that for fixed $\sigma$ and $N_A$, the profiles of $\langle\theta\rangle$ are almost identical independent of the chain length $N_{br}$ or $\langle N_{br}\rangle$. The transition point and the transition width are identical.

The universality of the transition points is clearly shown in Figure 8. As expected, the transition points are essentially

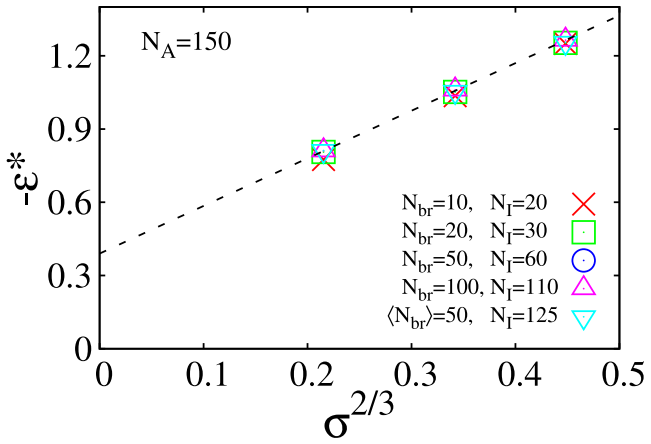


**Figure 8.** Transition point of single diblock copolymer chains in monodisperse and polydisperse brushes with fixed $N_{br}$ and $N_I$ as a function grafting density. The active block length is set at $N_A = 150$. The dashed line shows the function $1.95 \cdot x + 0.39$.

independent of the brush chain length and the brush polydispersity if $N_I$ is sufficiently long. From the data, we learn that even for very short brush chains, e.g., $N_{br} = 10$, the results are still valid. The transition point ($-\varepsilon^*$) increases with $\sigma$ according to a power law. This can be analyzed according to the mean field theory,[29] which gives $\varepsilon^* \propto \mu^{-1}(V_0)$ (see eq 10), where $V_0 \propto \sigma^{2/3}$. As already discussed in Theoretical Consideration, the explicit expression of $\mu^{-1}$ depends on the specific form of the adsorption potential;[30,31] here, we consider the situation for large $V_0$. In this case, theoretical consideration predicts that $\mu^{-1}(x) \approx x$, leading to $-\varepsilon^* \propto \sigma^{2/3}$, which matches the fitting curve in Figure 8 well.

Next, we investigate the finite chain length effect of $N_A$. Figure 9 compares $\langle\theta\rangle$ as a function of $-\varepsilon$ for two sticky block lengths $N_A = 100$ and $N_A = 400$ in monodisperse and polydisperse brushes. As already discussed, for fixed $N_A$ and $\sigma$, the profiles of $\langle m\rangle$ collapse into a single master curve independent of the brush chain polydispersity. If $N_A$ is large, then $\langle\theta\rangle$ becomes sharper. It thus can be expected that when $N_A$ approaches infinity, $\langle\theta\rangle$ becomes a step function, implying a first-order transition in the thermodynamic limit. For a finite value of $N_A$, the transition is smeared out. For $N_A = 400$, the theoretical curve gives an excellent match to the simulation results, while for the shorter sticky block, logarithmic corrections become relatively more important, leading to a small shift in the transition point as well as small discrepancies away from the transition.

Figure 10 plots two sets of the nonequilibrium free energy function $U(m)$ at the transition point. For both $N_A = 100$ and $N_A = 200$, the corresponding set of curves for different brush


https://dx.doi.org/10.1021/acs.macromol.0c02095
Macromolecules 2021, 54, 2592−2603

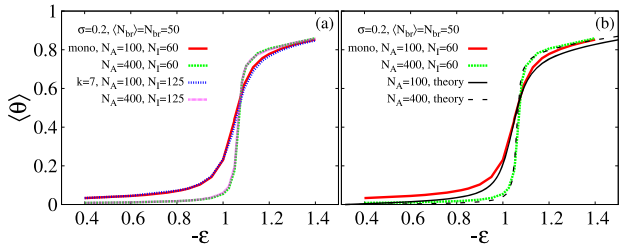


**Figure 9.** Average fraction of number of contact for different structures of diblock copolymer switches (a) and comparison with theoretical predictions (b). The length of the inert block is chosen to be sufficiently long compared to that of the brush chains. The length of the monodisperse brush chains is set equal to the number-average length of polydisperse brush chains $N_{br} = \langle N_{br} \rangle$. The grafting density is $\sigma = 0.2$. The black continuous line and dotted line give the results, respectively, for $N_A = 100$ and $N_A = 400$ from eq 13. For $N_A = 100$, we take $\varepsilon^* = -1.04$ and, thus, $\theta_{homo}(\varepsilon^*) = 0.770$, and in the case of $N_A = 400$, we take $\varepsilon^* = -1.06$ and, thus, $\theta_{homo}(\varepsilon^*) = 0.776$.

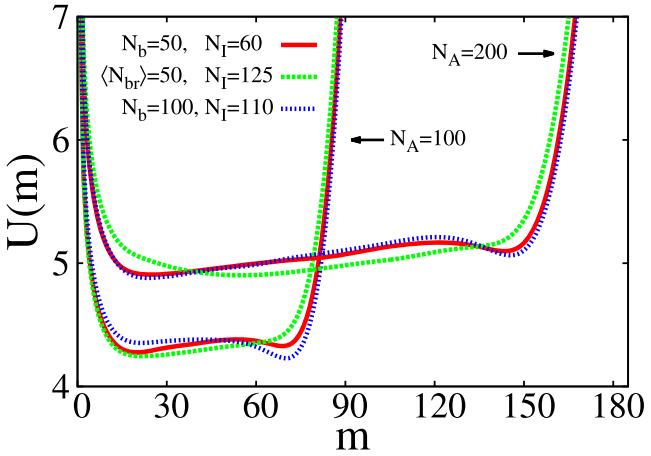


**Figure 10.** Landau free energy as a function of $m$ with $N_A = 100$ at $\varepsilon^* = -1.048$ and $N_A = 200$ at $\varepsilon^* = -1.055$ for different lengths of brush chains and $N_I$ as denoted. The grafting density is $\sigma = 0.2$.

lengths and polydispersities are approximately the same. The wide flat region appearing in $U(m)$ demonstrates the coexistence of the two equilibrium states without any energy barrier between them. The corresponding value of $(-\varepsilon)$ defines the transition point. For $N_A = 100$, the transition point for the three different setups in Figure 10 is the same, $\varepsilon^* \approx -1.048$, and for $N_A = 200$, it is $\varepsilon \approx -1.055$. Therefore, the transition point shifts only slightly for different $N_A$. We should note that in some of these curves, a very small energy barrier can be seen, which may be due to the logarithm corrections. However, these barriers are totally insignificant in relation to the kinetic aspects of the switching transition as they are far below the thermal energy $k_B T$.

**Equivalence between the External Pulling Force and the Brush-Induced Repulsion.** The conformational transition of the single grafted active polymer is determined by the interplay between the substrate adsorption and brush-induced osmotic repulsion. The tearing force that pulls the adsorbed monomers away from the substrate arises from the repulsion force acting on all the torn-off monomers. For the diblock copolymer switches under consideration, the inert block is always set sufficiently long such that during the phase transitions, a complete stem exists in the brush, which contributes a constant tearing force. From the point of view of the polymers, they cannot distinguish between different origins of the tearing force. Therefore, it is reasonable to expect that the phase behavior of a single grafted active homopolymer chain subjected to an external force at the free end (without a brush) is identical to that of a diblock copolymer with an active block and an inert block in a brush in the case where the both blocks are sufficiently long.

To test this, we run MC simulations for two different sets of systems. For the first set, we consider a diblock copolymer chain with $N_A = 100$ and $N_I = 60$ in a monodisperse brush with $N_{br} = 50$ and $\sigma = 0.1$,0.2, and 0.3. The other set contains a single grafted active homopolymer chain of the same length as $N_A$. A constant external force is imposed on the free end bead of this homopolymer. The simulations are done as follows. First, we run simulation for the diblock copolymer switches and, for each grafting density, we calculate the average number of contact as a function of adsorption strength. These results are shown in Figure 11 by three continuous curves. In the

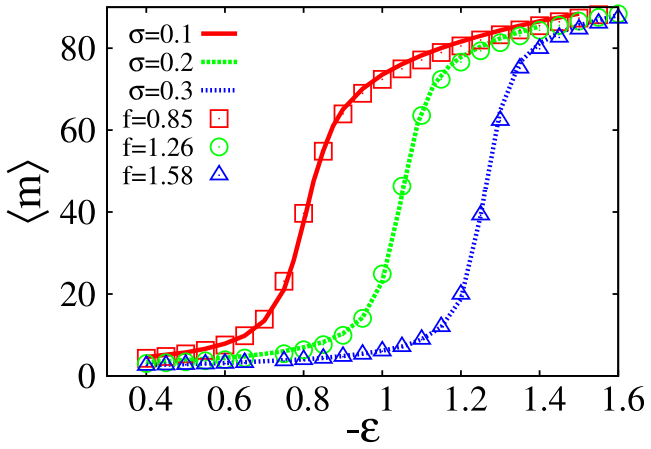


**Figure 11.** Comparison of the average number of contacts of diblock copolymer switches with $N_A = 100$, $N_I = 60$, and $N_{br} = 50$ in monodisperse brushes at grafting density $\sigma$ (lines) with those of single homopolymers on a bare substrate subject to an external force $f$ acting on the free end (symbols). The length of the homopolymer is set equal to the length of the active block of the diblock copolymer chain.

second step, we run simulations for the brush-free homopolymer switches. The average number of contact is also evaluated. The external force is adjusted by a trial-and-error method in such a way that the resulting curves for $\langle m \rangle$ are as close as possible to the curve obtained from the diblock copolymer switches.

From Figure 11, it can be seen that for each grafting density, there always exists an equivalent force $F$ for which the profile $\langle m \rangle$ across the adsorption transition perfectly matches that from the diblock copolymer switches. The good overlap demonstrates the equivalence of the phase transitions between these two sets of switches.

*SCF Analytical Theory.* Each monomer of the inert block experiences an outward force due to the gradient of the effective field. The mechanical balance condition relates this force to the variation of the local tension as follows[47]

$$\frac{d}{dn}\left(3\frac{dz}{dn}\right) - \frac{dV}{dz}z(n) = 0 \tag{18}$$

where $z(n)$ is the position of the $n$-th monomer, and the index $n$ is counted from the adsorbing surface. Integrating the forces


https://dx.doi.org/10.1021/acs.macromol.0c02095
Macromolecules 2021, 54, 2592−2603

over all the monomers located within the brush profile gives the natural result that the net outward force is balanced by the tension in the bond located exactly at the substrate

$$-\int_0^{n_{edge}} \frac{dV}{dz} z(n) dn = 3\frac{dz}{dn}\bigg|_{n=0} \tag{19}$$

since the tension at the outer brush edge, $3\frac{dz}{dn}\big|_{n=n_{edge}}$, vanishes. The balance equation has a first integral of the form $\frac{3}{2}\left(\frac{dz}{dn}\right)^2 - V(z) = \text{const}$, which has a simple conservation of energy interpretation within the analogy between the stretched chain conformation and a trajectory of a classical particle in the potential of $-V(z)$.[32] At the outer brush edge, both the chain tension and the effective potential are zero, which sets the value of the integration constant and leads to the final result for the net tearing force $f$

$$f = 3\frac{dz}{dn}\bigg|_{n=0} = \sqrt{6V(0)} \tag{20}$$

It is important that the inert block is longer than the brush chains and is guaranteed to extend to the outer edge of the brush. However, the monomers that reside entirely outside the brush do not contribute to the outward tearing force and, in that sense, the actual length of the inert block is also irrelevant, provided that the above condition is satisfied. The SCF theory gives that $V(0) = \frac{3}{2}\left(\frac{\pi}{2}\nu\sigma\right)^{2/3}$ ($V(0) = V_0$). Thus, the tearing force is given by

$$f = 3\left(\frac{\pi}{2}\nu\sigma\right)^{1/3} \tag{21}$$

and depends neither on the length of the brush-forming chains nor on brush polydispersity. This is perfectly consistent with Figure 7, showing the adsorption curves to be perfectly insensitive to the brush parameters at fixed $\nu\sigma$.

Figure 12 displays the comparison of the force values obtained by matching the adsorption curves in the MC simulations with the prediction of the SCF theory (eq 21).

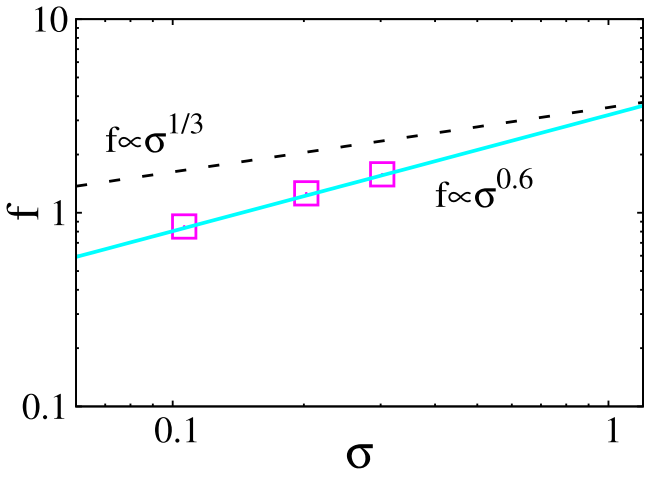


**Figure 12.** Equivalent tearing force as a function of the brush grafting density: fitting the MC adsorption curves (continuous line) in comparison to the analytical SCF theory of eq 21 (dashed line) with the excluded volume parameter setting at $\nu = 1$.

Clearly, the correlated fluctuations of the brush and the diblock chain result in a reduced average tearing force as opposed to the fixed repulsive field in the SCF picture, although the relative difference becomes smaller for denser brushes.

It is clear from the theoretical picture of the brush that is the generator of the tearing force that the strength of the force is independent of the length of the sticky block. This is illustrated in Figure 13, where the adsorption curves $\langle m\rangle(\varepsilon)$ for a homopolymer with an external force and for the diblock copolymer in a brush are superimposed, taking one and the same value of the external force $f = 0.68$ for several values of $N_A$.

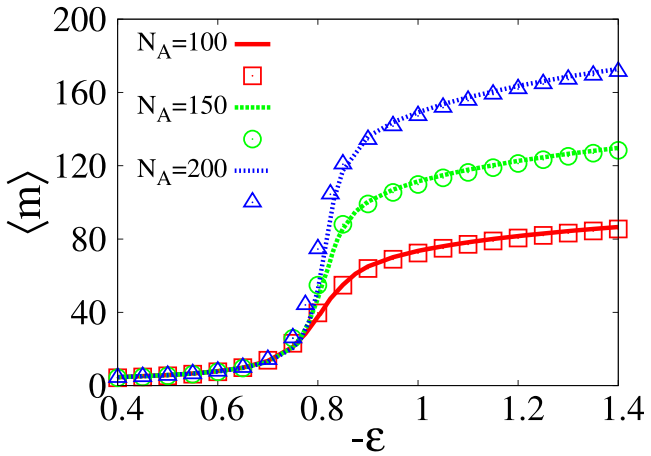


**Figure 13.** Average number of contact obtained from diblock copolymer switches in monodisperse brushes with $N_I = 60$ and $N_{br} = 50$ (lines) and from single homopolymer switches without a brush (symbols) with a fixed force imposed on the free end monomer ($f = 0.85$). The length of the homopolymer is set equal to the length of the active block of the diblock copolymer chain.

**Anomalous Contact Number Fluctuations.** To further investigate the transition properties of diblock copolymer switches, we finally examine the fluctuations of the number of contact, which is defined as $\langle(\delta m)^2\rangle \equiv \langle m^2\rangle - \langle m\rangle^2$.

Figure 14 presents the $\langle(\delta m)^2\rangle$ as a function of $-\varepsilon$ with different $N_A$. The maximum of $\langle(\delta m)^2\rangle$ gives another way to define the transition point. For different $N_A$, the transition point is slightly different due to the finite chain length effect; for example, we have $\varepsilon^* \approx -1.048$ for $N_A = 100$, $\varepsilon^* \approx -1.055$ for $N_A = 200$, and $\varepsilon^* \approx -1.066$ for $N_A = 400$. Below the transition point, $\langle(\delta m)^2\rangle$ increases by an inverse quadratic law $\langle(\delta m)^2\rangle \approx |-\varepsilon + \varepsilon^*|^{-2}$, and it diverges at the transition point $-\varepsilon = -\varepsilon^*$ in the infinite chain length limit $N_A \to \infty$. After crossing the transition point, the fluctuation decreases slowly, showing strong dependence over $N_A$. We assume that the fluctuation scales as $\langle(\delta m)^2\rangle \propto N_A^{\alpha}$, where $\alpha$ depends on the adsorption strength (see the inset of Figure 14). At weak adsorption, we obtain that $\alpha \simeq 0$ independent of $N_A$ covering a large $\varepsilon$ region. At the transition point, $\langle(\delta m)^2\rangle$ scales $N_A$ quadratically. At strong adsorption, the scaling component is about $\alpha \simeq 1$.

In analogy to the average number of contact, the fluctuation $\langle(\delta m)^2\rangle$ also shows universal properties that if the length of the active block $N_A$ and the grafting density are the same, then the profiles of $\langle(\delta m)^2\rangle$ obtained with respect to $-\varepsilon$ are identical independent of the detailed structures of the brush (data not shown).


https://dx.doi.org/10.1021/acs.macromol.0c02095
Macromolecules 2021, 54, 2592−2603

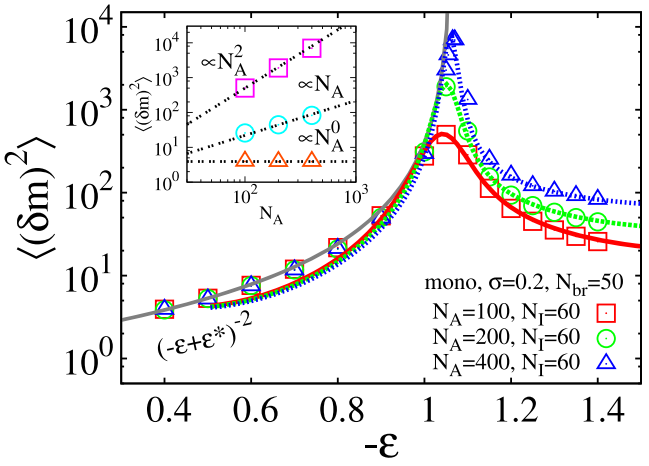


**Figure 14.** Fluctuation of number of contact as a function of adsorption strength $-\varepsilon$ for diblock copolymer switches in a monodisperse brush with polymer and brush parameters as noticed. The continuous gray line corresponds to a fit of the data for $\langle(\delta m)^2\rangle$ below the transition point. The inset shows the dependence of $\langle(\delta m)^2\rangle$ on $N_A$ at the region of weak adsorption and at critical adsorption and strong adsorption of $\varepsilon = -1.4$. Dashed lines in the inset are obtained as fits to the data of $\langle(\delta m)^2\rangle$. Colored continuous lines present the analytical predictions from eq 15. For $N_A$ = 100,200, and 400, we take $\varepsilon^* = -1.04$, $-1.05$, and $-1.06$, respectively.

The critical divergence of $\langle(\delta m)^2\rangle$ at the transition point has a close relation with the critical slowdown behavior, and this has a significant effect on the switching time. For conventional first-order transitions, the switching time is determined by the energy barrier according to the Arrhenius formula.[48] In contrast, barrier-free transitions at the transition point are controlled by diffusion-type processes. The switching time is of the order of the relaxation time of the active block. If we suppose that the diffusion constant is inversely proportional to $N_A$, the switch time then can be estimated as a power law to scale as $\tau \propto N_A^{\beta}$, where $\beta$ is around 3. The relation between the anomalous fluctuations and the slowing down of the relaxation process for an isolated adsorbing homopolymer with a fixed external end-force applied were studied in detail before by Brownian dynamics simulations.[27] Because of the very close similarity between the block-copolymer in a brush and a homopolymer with an external force applied, these results are relevant to the problem discussed here.

## DISCUSSION AND OUTLOOK

The main purpose of the current work was to evaluate the performance and robustness of a type of multicomponent brush switch, which contains grafted adsorption-responsive minority chains in an otherwise inert polymer brush. In these switches, sharp barrier-free transitions between states are possible, which should be interesting for applications in the design of sensors and smart surfaces.

We found that the barrier-free transitions are universal in the sense that if the active block and inert block are sufficiently long, then the transition behavior of different systems is essentially identical and independent of the details of the brush structure, such as the number-averaged chain length and polydispersity of the brush. This universality property facilitates the design of stable and controllable switch sensors in practice. Uncertainties in the production process that result in the "wrong" block lengths are predicted to have little influence on the main characteristics of the transition. We anticipate that the proposed picture is also valid for different types of brushes including curved, dendritic, or partially cross-linked brushes. Due to the high performance, high reliability, and strong robustness, we believe that the newly proposed switches should be interesting candidates for practical applications.

The analysis presented above essentially considers a single active chain surrounded by inert brush chains. It is natural to ask what would change if there is a finite concentration of active chains. One can identify several regimes according to the surface grafting density of active chains, $\sigma_A$. Long active blocks in the adsorbed state take flat, essentially 2D coil-like conformations of characteristic size $R_g \propto N_A^{3/4}$. So, at very low active chain grafting densities, $\sigma_A < N_A^{-3/2}$, the diblocks are truly isolated, and the single active chain approximation is fully justified. A regime with a moderate degree of active block overlap can be identified as $N_A^{-3/2} < \sigma_A < N_A^{-1}$. There appears some competition for adsorption sites between the neighboring active blocks, but the monomer density in the adsorption layer is still not too close to saturation. In this regime, we expect the switching transition to be somewhat modified but without any qualitative changes. Finally, the strong overlap regime is realized at $\sigma_A > N_A^{-1}$; here, the adsorbed state would carry an important additional free energy penalty due to strong crowding in the adsorption layer. The strong overlap regime is poorly understood. Diblock–diblock interaction could also take place in the desorbed state once the expelled tails start forming a secondary brush layer that would modify the desorbed state free energy and thus also affect the transition. The secondary brush regime appears under condition $\sigma_A > (N_A + N_A - N_{br})^{-2\nu}$, where $\nu \approx 3/5$ is the Flory index in three dimensions. However, the secondary brush, which is only marginally overlapping, introduces only a minor change in the chemical potential of the tail and is therefore of small importance. One can conclude that the breakdown of the switching transition picture we have presented above is largely brought by entering the strong overlap regime, $\sigma_A > N_A^{-1}$, for the active blocks.

On the side of fundamental theory, we have established an equivalence between the unusual phase transition in our system and the unusual phase transition in the mechanical desorption of isolated polymer chains induced by an external force. The latter transitions have been studied quite extensively (see, for example, refs 26 and 27). It was realized that in contrast to force-free adsorption, the transition becomes of first order and involves phase coexistence within a single macromolecule. However, for a flexible chain, the interface between the adsorbed and desorbed phases is reduced to one monomer and does not carry the interfacial free energy. As a result, there is no free energy barrier separating the coexisting phases, and one observes a power-law growth in fluctuations upon approaching the transition point, which is characteristic of the critical phenomena rather than the first order-type transitions. The question of whether these unusual phase transition features could be observed experimentally remained open. Indeed, experimental methods of single-chain manipulations include devices such as optical tweezers and superparamagnetic beads[49,50] that generate mechanical forces in the relevant range of several piconewtons. The difficulty lies in maintaining an exact fixed magnitude of the force: otherwise, the transition may be either smeared out or acquire an


https://dx.doi.org/10.1021/acs.macromol.0c02095
Macromolecules 2021, 54, 2592−2603

intermediate transition state with an associated free energy barrier.

Here, we have demonstrated that a constant tearing force appears naturally when a chain has a sufficiently long inert or desorbed tail threading the brush thickness and extending beyond its outer edge. The outward pulling force is generated by the brush density profile; importantly, the net force does not depend on any details of the profile and is solely determined by the difference in the mean force potential between the substrate and the free space outside the brush as seen in eq 20. According to the general theory, this potential difference is, in turn, determined by a single combination of the excluded volume parameter and the surface grafting density, $v\sigma$. The formula for the force applies as well to a special limit when the potential profile is reduced to a step function.[51] The step potential represents the situation when the force is concentrated at a sharply localized boundary between two regions. The same effect applies when the chain is partially confined in a tube or a slit. Mechanically, the force is generated by collisions with the edge, while thermodynamically, it is related to the difference in free energies between the two regions, which may be due to the confinement entropy. Dynamic consequences of the constant pulling force generated when a chain is partially confined in a tube were demonstrated experimentally in refs 52 and 53 and in MC simulations54 and analyzed in view of possible chromatographic applications in ref 55. Any system that combines the naturally tail-generated pulling force with adsorption would be expected to demonstrate the unusual barrier-free, first order-type transition.

## AUTHOR INFORMATION


### Corresponding Author

**Shuanhu Qi** − *Key Laboratory of Bio-inspired Smart Interfacial Science and Technology of Ministry of Education, School of Chemistry, Beihang University, Beijing 100191, China;* orcid.org/0000-0002-4260-4641; Email: qishuanhu@buaa.edu.cn

### Authors

**Leonid I. Klushin** − *Department of Physics, American University of Beirut, Beirut 1107 2020, Lebanon; Institute for Macromolecular Compounds RAS, 1199004 St. Petersburg, Russia*

**Alexander M. Skvortsov** − *Chemical-Pharmaceutical University, 197022 St. Petersburg, Russia*

**Friederike Schmid** − *Institut für Physik, Johannes Gutenberg-Universität Mainz, D-55099 Mainz, Germany;* orcid.org/0000-0002-5536-6718

Complete contact information is available at: https://pubs.acs.org/10.1021/acs.macromol.0c02095


### Notes

The authors declare no competing financial interest.

## ACKNOWLEDGMENTS

Financial support by the National Natural Science Foundation of China (NSFC) through grant 21873010 and through collaborative grant NNIO-a 20-53-12020 funded jointly by the Russian Foundation for Basic Research (RFBR) and the Deutsche Forschungsgemeinschaft (DFG) and also by the DFG through grants Schm 985/13-2 and SFB TRR 146 (project C1) is gratefully acknowledged. Simulations have been performed on the computer cluster at Beihang University.

## REFERENCES


(1) Halperin, A.; Tirrell, M.; Lodge, T. P. Tethered chains in polymer microstructures. *Adv. Polym. Sci.* **1992**, *100/1*, 31−71.

(2) Milner, S. T. Polymer Brushes. *Science* **1991**, *251*, 905−914.

(3) Advincula, R. C. *Polymer brushes;* Wiley: Weinheim, 2004.

(4) Motornov, M.; Minko, S.; Eichhorn, K.-J.; Nitschke, M.; Simon, F.; Stamm, M. Reversible tuning of wetting behavior of polymer surface with responsive polymer brushes. *Langmuir* **2003**, *19*, 8077−8085.

(5) Sheparovych, R.; Motornov, M.; Minko, S. Adapting low-adhesive thin films from mixed polymer brushes. *Langmuir* **2008**, *24*, 13828−13832.

(6) de Vos, W. M.; Biesheuvel, P. M.; de Keizer, A.; Kleijn, J. M.; Cohen Stuart, M. A. Adsorption of the protein bovine serum albumin in a planar poly(acrylic acid) brush layer as measured by optical reflectometry. *Langmuir* **2008**, *24*, 6575−6584.

(7) Motornov, M.; Sheparovych, R.; Lupitskyy, R.; MacWilliams, E.; Hoy, O.; Luzinov, I.; Minko, S. Stimuli-responsive colloidal systems from mixed brush-coated nanoparticles. *Adv. Funct. Mater.* **2007**, *17*, 2307−2314.

(8) Borukhov, I.; Leibler, L. Stabilizing grafted colloids in a polymer melt: Favorable enthalpic interactions. *Phys. Rev. E* **2000**, *62*, R41−R44.

(9) Jaquet, B.; Wei, D.; Reck, B.; Reinhold, F.; Zhang, X.; Wu, H.; Morbidelli, M. Stabilization of polymer colloid dispersions with pH-sensitive poly-acrylic acid brushes. *Colloid Polym. Sci.* **2013**, *291*, 1659−1667.

(10) Klein, J. Shear, friction, and lubrication forces between polymer-bearing surfaces. *Annu. Rev. Mater. Sci.* **1996**, *26*, 581−612.

(11) Desai, P. R.; Das, S. Lubrication in polymer-brush bilayers in the weak interpenetration regime: Molecular dynamics simulations and scaling theories. *Phys. Rev. E* **2018**, *98*, No. 022503.

(12) Zhulina, E. B.; Leermakers, F. A. M.; Borisov, O. V. Structure and lubrication of solvent-free dendron brushes. *Polymer* **2017**, *120*, 223−235.

(13) Mura, S.; Nicolas, J.; Couvreur, P. Stimuli-responsive nanocarriers for drug delivery. *Nat. Mater.* **2013**, *12*, 991−1003.

(14) Papaphilippou, P.; Loizou, L.; Popa, N. C.; Han, A.; Vekas, L.; Odysseos, A.; Krasia-Christoforou, T. Superparamagnetic hybrid micelles, based on iron oxide nanoparticles and well-defined diblock copolymers possessing $\beta$-ketoester functionalities. *Biomacromolecules* **2009**, *10*, 2662−2671.

(15) Stuart, M. A. C.; Huck, W. T. S.; Genzer, J.; Müller, M.; Ober, C.; Stamm, M.; Sukhorukov, G. B.; Szleifer, I.; Tsukruk, V. V.; Urban, M.; Winnik, F.; Zauscher, S.; Luzinov, I.; Minko, S. Emerging applications of stimuli-responsive polymer materials. *Nat. Mater.* **2010**, *9*, 101−113.

(16) Draper, J.; Luzinov, I.; Minko, S.; Tokarev, I.; Stamm, M. Mixed polymer brushes by sequential polymer addition: anchoring layer effect. *Langmuir* **2004**, *20*, 4064−4075.

(17) Merlitz, H.; He, G.-L.; Wu, C.-X.; Sommer, J.-U. Nanoscale brushes: how to build a smart surface coating. *Phys. Rev. Lett.* **2009**, *102*, 115702.

(18) Romeis, D.; Sommer, J.-U. Conformational switching of modified guest chains in polymer brushes. *J. Chem. Phys.* **2013**, *139*, No. 044910.

(19) Akkilic, N.; Leermakers, F. A. M.; de Vos, W. M. Responsive polymer brushes for controlled nanoparticle exposure. *Nanoscale* **2015**, *7*, 17871−17878.

(20) Koch, M.; Romeis, D.; Sommer, J.-U. End-adsorbing chains in polymer brushes: pathway to highly metastable switchable surfaces. *Macromolecules* **2020**, *53*, 7356.

(21) Klushin, L. I.; Skvortsov, A. M.; Polotsky, A. A.; Qi, S.; Schmid, F. Sharp and fast: sensors and switches based on polymer brushes with adsorption-active minority chains. *Phys. Rev. Lett.* **2014**, *113*, No. 068303.

(22) Qi, S.; Klushin, L. I.; Skvortsov, A. M.; Liu, M.; Zhou, J.; Schmid, F. Tuning transition properties of stimuli-responsive brushes by polydispersity. *Adv. Funct. Mater.* **2018**, *28*, 1800745.

(23) Qi, S.; Klushin, L. I.; Skvortsov, A. M.; Polotsky, A. A.; Schmid, F. Stimuli-responsive brushes with active minority components: Monte Carlo study and analytical theory. *Macromolecules* **2015**, *48*, 3775−3787.
(24) Skvortsov, A. M.; Klushin, L. I.; Gorbunov, A. A. Long and short chains in a polymeric brush: a conformational transition. *Macromolecules* **1997**, *30*, 1818−1827.
(25) Skvortsov, A. M.; Gorbunov, A. A.; Leermakers, F. A. M.; Fleer, G. J. Long minority chains in a polymer brush: a first-order adsorption transition. *Macromolecules* **1999**, *32*, 2004−2015.
(26) Klushin, L. I.; Skvortsov, A. M. Unconventional phase transitions in a constrained single polymer chain. *J. Phys. A: Math. Theor.* **2011**, *44*, 473001.
(27) Zhang, S.; Qi, S.; Klushin, L. I.; Skvortsov, A. M.; Yan, D.; Schmid, F. Anomalous critical slowdown at a first order phase transition in single polymer chains. *J. Chem. Phys.* **2017**, *147*, No. 064902.
(28) Zhang, S.; Qi, S.; Klushin, L. I.; Skvortsov, A. M.; Yan, D.; Schmid, F. Phase transitions in single macromolecules: Loop-stretch transition versus loop adsorption transition in end-grafted polymer chains. *J. Chem. Phys.* **2018**, *148*, No. 044903.
(29) Qi, S.; Klushin, L. I.; Skvortsov, A. M.; Schmid, F. Using copolymers to design tunable stimuli-reponsive brushes. *Macromolecules* **2020**, *53*, 5326−5336.
(30) Grassberger, P. Simulations of grafted polymers in a good solvent. *J. Phys. A: Math. Gen.* **2005**, *38*, 323−331.
(31) Klushin, L. I.; Polotsky, A. A.; Hsu, H.-P.; Markelov, D. A.; Binder, K.; Skvortsov, A. M. Adsorption of a single polymer chain on a surface: Effects of the potential range. *Phys. Rev. E* **2013**, *87*, No. 022604.
(32) Milner, S. T.; Witten, T. A.; Cates, M. E. Effects of polydispersity in the end-grafted polymer brush. *Macromolecules* **1989**, *22*, 853−861.
(33) Zhulina, E. B.; Borisov, O. V.; Priamitsyn, V. A. Theory of steric stabilization of colloid dispersions by grafted polymers. *J. Colloid Interface Sci.* **1990**, *137*, 495−511.
(34) Qi, S. Particle penetration into polydisperse polymer brushes: A theoretical analysis. *Macromol. Theory Simul.* **2017**, *26*, 1700029.
(35) Yuan, F.; Wang, S.; Larson, R. G. Potentials of mean force and escape times of surfactants from micelles and hydrophobic surfaces using molecular dynamics simulations. *Langmuir* **2015**, *31*, 1336−1343.
(36) Balazs, A. C.; Singh, C.; Zhulina, E.; Lyatskaya, Y. Modeling the phase behavior of polymer/clay nanocomposites. *Acc. Chem. Res.* **1999**, *32*, 651−657.
(37) Laradji, M.; Guo, H.; Zuckermann, M. J. Off-lattice Monte Carlo simulation of polymer brushes in good solvents. *Phys. Rev. E* **1994**, *49*, 3199−3206.
(38) Besold, G.; Guo, H.; Zuckermann, M. J. Off-lattice Monte Carlo simulation of the discrete Edwards model. *J. Polym. Sci., Part B: Polym. Phys.* **2000**, *38*, 1053−1068.
(39) Schulz, G. V. *Z. Phys. Chem.* **1939**, *43*, 25−46.
(40) Zimm, B. H. Apparatus and methods for measurement and interpretation of the angular variation of light scattering; preliminary results on polystyrene solutions. *J. Chem. Phys.* **1948**, *16*, 1099−1116.
(41) Rubinstein, M.; Colby, R. H. *Polymer Physics;* Oxford University Press: Oxford, 2003.
(42) Detcheverry, F. A.; Kang, H.; Daoulas, K. C.; Müller, M.; Nealey, P. F.; de Pablo, J. J. Monte Carlo simulations of a coarse grain model for block copolymers and nanocomposites. *Macromolecules* **2008**, *41*, 4989−5001.
(43) Qi, S.; Klushin, L. I.; Skvortsov, A. M.; Schmid, F. Polydisperse polymer brushes: internal structure, critical behavior, and interaction with flow. *Macromolecules* **2016**, *49*, 9665−9683.
(44) Frenkel, D.; Smit, B. *Understanding Molecular Simulation: From Algorithms to Applications*; Academic Press: New York, 2001.
(45) de Vos, W. M.; Leermakers, F. A. M. Modeling the structure of a polydisperse polymer brush. *Polymer* **2009**, *50*, 305−316.
(46) Klushin, L. I.; Skvortsov, A. M.; Qi, S.; Schmid, F. Polydisperse Brush with the Linear Density Profile. *Polym. Sci., Ser. C* **2018**, *60*, 84−94.
(47) Milner, S. T.; Witten, T. A.; Cates, M. E. Theory of the grafted polymer brush. *Macromolecules* **1988**, *21*, 2610−2619.
(48) Paul, W.; Baschnagel, J. *Stochastic Processes: From Physics to Finance;* Springer: Berlin, 1999.
(49) Moffitt, J. R.; Chemla, Y. R.; Smith, S. B.; Bustamante, C. Recent advances in optical tweezers. *Annu. Rev. Biochem.* **2008**, *77*, 205−228.
(50) Smith, S.; Finzi, L.; Bustamante, C. Direct mechanical measurements of the elasticity of single DNA molecules by using magnetic beads. *Science* **1992**, *258*, 1122−1126.
(51) Skvortsov, A. M.; Klushin, L. I.; van Male, J.; Leermakers, F. A. M. First-order coil-to-flower transition of a polymer chain pinned near a stepwise external potential: numerical, analytical, and scaling analysis. *J. Chem. Phys.* **2001**, *115*, 1586.
(52) Turner, S. W. P.; Cabodi, M.; Craighead, H. G. Confinement-induced entropic recoil of single DNA molecules in a nanofluidic structure. *Phys. Rev. Lett.* **2002**, *88*, 128103.
(53) Levy, S. L.; Craighead, H. G. DNA manipulation, sorting, and mapping in nanofluidic systems. *Chem. Soc. Rev.* **2010**, *39*, 1133−1152.
(54) Milchev, A.; Klushin, L.; Skvortsov, A.; Binder, K. Ejection of a polymer chain from a nanopore: theory and computer experiment. *Macromolecules* **2010**, *43*, 6877−6885.
(55) Klushin, L.; Milchev, A.; Skvortsov, A. Efficient separation of long polymer chains by contour length and architecture. *ACS Macro Lett.* **2013**, *2*, 879−881.


https://dx.doi.org/10.1021/acs.macromol.0c02095
*Macromolecules* 2021, 54, 2592−2603